RÉNYI ENTROPY BASED SPECTRAL DESCRIPTORS FOR SAR IMAGE CONTENT RETRIEVAL

Anca POPESCU[1], Inge GAVĂȚ[2], Mihai DATCU

Această lucrare prezintă o metodă de măsura a conținutului informațional al reprezentării spectral Wigner-Ville a imaginilor Radar cu Apertura Sintetică (SAR), într-o abordare bazată pe imagete, care folosește măsura stohastică parametrică dată de Entropia Rényi. Pe baza conceptelor informaționale definite de Flandrin, se efectuează o analiză locală a reprezentării timp-frecvență a unei imagete SAR, rezultând într-o serie de descriptori ce pot fi folosiți pentru a identifica prezența unei anumite Categorii de Scenă într-o bază de date de imagete, şi de a regăsi imagetele cu conținut similar din perspectiva măsurii informaționale definite.

In this paper we measure the informational content of the Wigner-Ville spectral representation of SAR images in a patch-wise approach, making use of the parametric stochastic measure given by the Rényi Entropy. Following the informational measures defined by Flandrin, we perform a local analysis of the time-frequency representation of the SAR patch, resulting in a set of descriptors with further use to identify the presence of a given Scene Class in a patch database and to retrieve the patches that have similar content with respect to this specific informational measure.

Keywords: High Resolution SAR, Rényi Entropies, Image Classification

1. Introduction

With the increased interest in the usage of Synthetic Aperture Radar data for a variety of applications, and the growing number of spaceborne missions, there has been a constant interest in the understanding and modeling of the SAR system. From the information theory perspective, an interesting and key issue regarding the understanding of the SAR products was the amount of information that is contained in a SAR image. The analysis and interpretation of a SAR image is not a straightforward task to perform, due to the various physical and geometrical effects induced by the coherent acquisition mode and wave propagation factors. Measuring the information contained in a SAR image requires a good distinction between what is information and what is noise in a SAR product.

[1] PhD student, Faculty of Electronics, Telecommunications and Information technology, University POLITEHNICA o Bucharest, e-mail: ancaandreeapopescu@gmail.com

[2] Prof., Faculty of Electronics, Telecommunications and Information technology, University POLITEHNICA o Bucharest, e-mail: ancaandreeapopescu@gmail.com

Frost and Shanmugan [1] developed a statistical model for imaging radar systems, in which the radar system is considered as a noisy communication channel with multiplicative noise. Through the estimation of Mutual Information (MI), the authors evaluate the average amount of information that can be extracted about the imaged targets from the radar image. The analysis was made under the assumption that a resolution cell is made of a large number of scatterers (which applies for medium and low resolution images) and the received signal is modeled as a narrowband Gaussian random process. The average MI was defined as the rate at which information is transferred over a communication channel.

$$I(X,Y) = H(X) - H(Y \mid X) \tag{1}$$

where, X represents the imaged targets and Y the final radar image. The probability density function of X was modeled as a uniform distribution due to lack of a priori data. The experiments were conducted over SEASAT-A SAR images of 25 x 25 meters resolution and an equivalent number of looks N=3. An important remark of the paper was that the fundamental limitation on the information content is set by N. Later, in 2006, [2] used an information theoretic approach to model SAR images for change detection purposes. The authors derived a pixel feature for multi-temporal SAR image analysis from information theory concepts. The idea was that the negative of the logarithm of the probability of an amplitude level in one image conditional to the level of the same pixel in the other image would give an estimate of the degree of change occurred between passes. The topic of information content of SAR images was reiterated by Datcu in [3]. As a continuation of the work of [1], the authors proposed an approach suitable for high resolution images. The authors noted that for this kind of data it is difficult to correctly take into account the correlation between neighboring pixels due to the high resolution (meter, sub-meter) and stressed the importance of temporal and spatial correlation of speckle, following the work of [4]. The authors modeled the scene using a Gauss Markov Random Fields approach and emphasized the fact that both radiometric and spatial resolution have to be taken into account in order to completely define a measure of information content (i.e. MI). The SAR channel was modeled as a communication channel affected by a Gamma distributed multiplicative noise. The noise variance was proven to depend inversely proportional on the number of looks. Unlike [1], the probability density function of the scene is no longer considered uniform but instead is estimated through GMRF, taking into account the correlation between neighboring pixels (i.e. if a pixel is strongly different from its neighbors then it is more likely that it is a manifestation of noise, rather than a real variation of the scene reflectivity). The authors draw some interesting conclusions, among which the fact that the MI is an increasing function of the number of looks and that the urban areas have the

maximum value of MI, due to the increased heterogeneity compared to areas dominated by vegetation. Considering the definition of the MI, this last conclusion can be interpreted as the fact that an area with increased heterogeneity will have an increased value of the entropy. Entropy is a measure of the informational content of signals. The areas which are dominated by vegetation, with a pronounced uniform and homogeneous character, can be described by a small number of samples which means that the redundancy will be increased and the entropy will be lower. Conversely, the areas which contain various targets, especially man-made ones, will require longer descriptors, the redundancy will be lower and the entropy will have a larger value.

The scope of this paper is to try to verify whether or not entropy can be used as a feature for high resolution SAR image classification purposes. As an information measure, we will employ the generalized Rényi entropies. In literature, the entropy has been used in the analysis and processing of SAR images especially to improve the performances of classification schemes but also as a parameter or feature for classification [5], [6]. Moreover [7] used the entropy of the reflected signal in order to determine the randomness of the model of polarimetric SAR images built based on statistical parameters. The technique proposed by the authors is reiterated in [8] and used for an unsupervised classification of the types of landcover and man-made objects using as test data polarimetric SAR images.

The Rényi entropy as a descriptive measure was used in multimedia as well as in remote sensing applications. [9] use local directional Rényi entropy to build a local image descriptor for image feature extraction. The authors use entropy to measure the local saliency of images and define a descriptor with invariant properties to transformations such as translation, rotation, scale, illumination, occlusion, deformation and viewpoint variation and apply the method on multimedia images for object recognition purposes. The authors of [10] use the Rényi entropy as a similarity metric for clustering applications. In [11] the authors define a Jensen-Rényi based divergence measure for image registration purposes in inverse Synthetic Aperture Radar applications.

Throughout this paper we will employ the Rényi entropy as an information measure and a descriptor of SAR images, in an approach that takes into account the context of high resolution SAR scenes. When resolution increases up to meter resolution, a pixel level analysis does not offer sufficient information to distinguish the various scene categories, especially for the case of images which contain urban and man-made elements. This is why we will use an image analysis method in a localized approach with an extended analysis window; such that the size can ensure that the context details are being captured, thus helping to a better understanding of the scene content.

The analysis window is set to a size of 200 x 200 pixels and sweeps the entire scene and decomposes it into patches of equal size. Next, the analysis is performed locally, in a patch-based manner. However, we do take into account the non-stationary character of the SAR signal within a patch. For this reason, the Rényi entropy will be used as an estimate of the informational content and complexity of the time-frequency (TF) representation of each patch.

2. The Rényi Entropy. Theoretical Considerations

Information theory provides a measure of uncertainty or entropy that can be maximized mathematically to find the probability distribution that is maximally unbiased. Maximum entropy in terms of Shannon entropy is given by:

$$\begin{cases} \max(H(X)) = -\sum_{i\geq 1} p_i \log(p_i) \\ C(X) = \text{constraints} \end{cases}, with \quad \sum_{i\geq 1} p_i = 1 \tag{2}$$

The system under test is the scene imaged by a SAR system. Given the complete randomness of the input, no constraint is known a priori. In the expression given above, p_i denotes a probability, in terms of probability distributions, that is subject for evaluation (what is the best estimate $\hat{p}_i$ so that $H(X)$ is maximized) [12]. Thus, we estimate the TF representation of the SAR image and we substitute the probability distribution with the Wigner-Ville spectrum normalized so that $\sum_{i\geq 1} p_i = 1$.

This paper focuses on the application of entropy measures to TF representations (TFRs) to measure the complexity and information content of the non-stationary SAR signal via the TF plane. Given the negative values taken on by most TFRs, the Shannon entropy as described by (2) cannot be applied. In [13] a thorough study on the possibilities of measuring signal complexity and information content based on entropies, shows that the Rényi entropy can be used for this kind of applications.

$$H_\alpha(C_s) = -\iint C_s(t,f)\log_2(C_s(t,f))dtdf \tag{3}$$

$$H_\alpha(C_s) = \frac{1}{1-\alpha}\log_2 \iint C^\alpha{}_s(t,f)dtdf \tag{4}$$

In information theory, the Rényi entropy is an extension of Shannon's entropy through the relaxation of the additivity constraint. The Rényi entropy, named after Alfred Rényi, is one of a family of functionals for quantifying the diversity, uncertainty or randomness of a system:

$$H_\alpha(C_s) = \frac{1}{1-\alpha} \ln \sum_{i=1}^{N} p_i^\alpha \tag{5}$$

In the above equation the parameter α is greater or equal to 0 and it becomes obvious that when α=1 the Rényi entropy tends to the Shannon entropy. For a random variable X taking values with probabilities given by the *p* series, the Rényi entropy is a continuous positive decreasing function of α. In addition to appearing immune to the negative TFR values, the third order Rényi entropy measures signal complexity. The restrictions for α and C_s (the joint TF function that indicates how the frequency content of a signal s changes over time) are given in [13]. Also, the third order Rényi entropy is well defined for large classes of signals and TFRs. The most important properties of these entropies are:

1. Component counting – a two component signal $s+T_s$ contains exactly one bit more information than the one component signal s: $H_\alpha(I_{s+T_s}) = H_\alpha(I_S) + 1$
2. Invariance to TF representations (such as the Wigner Ville representation employed here) cross-terms interferences;
3. Amplitude and phase sensitivity (amplitude discrepancies alter the asymptotic saturation level of the Rényi entropy, while phase offsets induce strong oscillations between saturation levels);
4. Invariance to information-invariant signal transformations;
5. Boundaries: lower bound given by a single Gaussian pulse;
6. Dimensions (for simple signals composed of disjoint, equal amplitudes of one basic function, the Rényi dimension counts the number of components).

Proofs of the above listed properties are given in [13]. In the next section we will revise some of the fundamental properties of the Wigner-Ville TF representation of non-stationary signals and we will discuss the applicability of the Rényi entropy over TFRs to measure complexity.

3. Wigner-Ville Time-Frequency Representation

The Fourier analysis, although very useful for the study of stationary signals with invariant properties over time, is inadequate for non-stationary signals for which TF representations resolve issues like the change of wavenumber with space and of frequency with time, and generally allow for the investigation of signal properties in both the space and the wave number domains.

The use of the Wigner distribution for TF analysis of non-stationary signals provides a great advantage compared to other methods, due to the precision of the spectral evolution localization, though the presence of interference terms may make the interpretation difficult. The Wigner-Ville distribution is defined as:

$$W_x(t,f) = \int_{-\infty}^{\infty} x(t+\tau/2)x^*(t-\tau/2)e^{-j2\pi ft}d\tau \quad (6)$$

The WVD is a functional that keeps the time and frequency shifts and satisfies the marginals. An interpretation of (5) can be given in terms of probability distributions: (5) is the Fourier transform of the energy function of the signal. The most important properties of the Wigner distribution are given below (a more detailed description is given in [14]):

1. Energy preservation (by integrating the WV of a signal in the TF plane one gets the signal's energy) : $E_x = \iint W_x(t,f)dtdf$
2. Marginals (the energy spectral density and the instantaneous power can be obtained as marginal distributions of WV) : $\begin{cases} \int W_x(t,f)dt = \mid X(f) \mid^2 \\ \int W_x(t,f)df = \mid x(f) \mid^2 \end{cases}$
3. Real values
4. Covariance translation in time-and frequency
5. Filtering compatibility (if $y = x * h$ then $WWD(y) = WWD(x) * WWD(h)$, where * denotes time convolution)
6. Modulation compatibility (if y is obtained by modulating x with a function m then $WWD(y) = WWD(x) * WWD(m)$, where * denotes frequency convolution)
7. Interference (The WD computation of a multi-component signal introduces spurious "cross- terms" due to its intrinsic bi-linearity)

The Wigner Distribution might be interpreted as a local or regional spatial frequency representation of an image. It presents two main advantages with respect to other local representations. First, the WD is a real valued function and encodes directly the Fourier phase information. Second, the election of the appropriate window size, which depends on the kind of analyzed information, is not required for the computation of the WD. The WD of a 2-D image is a 4-D function that involves Fourier transformation for every point of the original image. The WD doubles the number of variables of the represented image. In this way, the WD of 2-D images is a 4-D function (2 spatial coordinates and 2 spatial-frequency coordinates). The most of the applications of the WD in image processing have been carried out through digital implementations. The definition of the discrete 4-D Wigner Distribution is given by (7).

$$W_f(n_x,n_y,m_u,m_v) = 2\sum_{k_x=-N/2}^{N/2-1}\sum_{k_y=-N/2}^{N/2-1} r_f(n_x,n_y,k_x,k_y)\cdot\exp\{-2j[(\frac{2\pi m_u}{N})k_x + (\frac{2\pi m_v}{N})k_y]\} \quad (7)$$

In (6), the term $r_f(n_x, n_y, k_x, k_y)$ denotes the product between the shifted image (vertically and horizontally by k_x, k_y) and its 180° rotation: $f(n_x + k_x, n_y + k_y)$ and $f^*(n_x - k_x, n_y - k_y)$.

In [12] was showed that a pixel level analysis based on the Rényi entropy of the TF representation of a square window centered on the current pixel can offer information regarding the structure of the image. The method captured the main targets visible in the image and offered information about the statistic of the analyzed scene. One of the conclusions of the paper was that the size of the analysis window contributes to the estimation performances. A larger analysis window led to better results. This can be explained by the fact that the text data had an increased resolution of a few meters and a pixel level analysis could not capture content and context information. Moreover, the analyzed data was composed of detected images, having only amplitude information. In this paper we will take into account these conclusions and we will extend the method proposed in [12]. First of all, the analysis will be performed on a larger window that will respond to the requirements of the high resolution data content. The analyzed scene contains both homogeneous areas, dominated by vegetation, water courses and water bodies, as well as urban areas where the objects are very diverse and the propagation mechanisms and geometrical effects are strongly visible. Using a patch-based approach (patches are obtained by applying a regular grid over the scene), we will try to understand how the entropy of the TF representation of a patch can be used as a descriptor of a given region in the scene. We will show that it can be an important parameter for SAR image indexing, being able to discriminate between different types of scene contents. Moreover, we consider two cases for comparison: one in which we use only the amplitude information if the image, where the speckle statistic has to be taken into account, and one in which the complex SAR signal in employed, where we can make use both of the amplitude and of the phase of the SAR signal.

4. Feature extraction procedure

For the analysis we have employed meter resolution TerraSAR-X data acquired in High Resolution Spotlight mode (~1m resolution) over Bucharest. The input data is composed of the Single Look Complex image for the first approach the detected version (amplitude representation) of the image for the second approach, and the complex interferogram for the third approach. The database description was detailed in the previous chapter. Due to the fact that the area covered by the interferometric data does not map the exact area covered by the SLC and detected data due to co-registration, and in order to reduce the computational time, we performed the analysis on a reduced set of interferometric

patches. Thus, the number of classes identified in the interferometric database is smaller than the number of classes identified in the complex and detected databases. The input data is approximately 10.000 x 6000 pixels, covering a great part of the city and including a large number of scene classes, from urban elements that form residential areas, business centers, bridges, industrial sites, and sport fields, to natural landscape like parks, water basins and courses, and so on. Over the original image we apply a regular grid and break the data into non-overlapping patches of 200 x 200 pixels. Thus we obtain a consistent patch database which will be used in the following processing steps. Over each patch we compute the Wigner-Ville spectrum which is normalized to meet the requirements of a probability distribution. Next, the α-parameterized Rényi entropy is computed for each patch and normalized for clustering purposes. The α parameter was set in turn to take the values 3, 5 and 7. For each patch we obtain thus a single value of the Rényi entropy parameter. The values are used to form a coefficients map which is classified in the final step, and thus a scene class map is generated, from which class masks can be extracted. The map quality is assessed through visual inspection by an image analyst, comparing optical image information with the generated class masks.

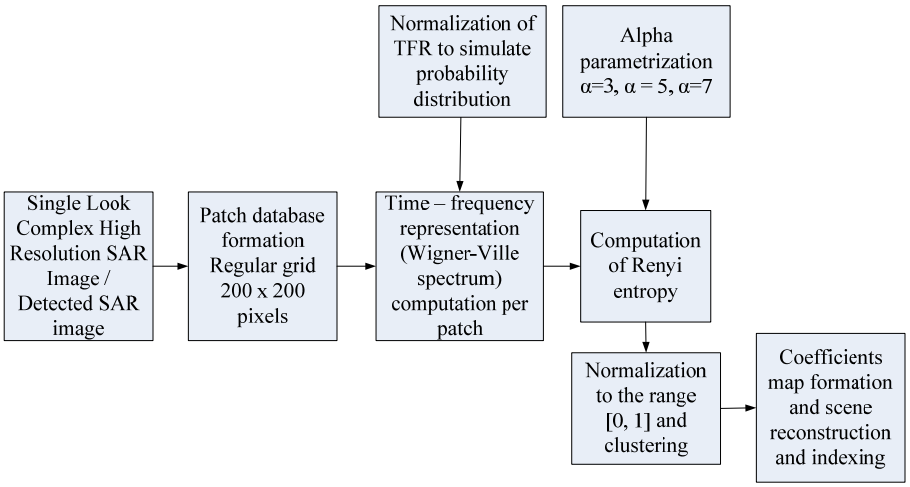

Fig.1. Feature extraction

Feature extraction is described in Fig 1: for the first approach the input data is formed of meter resolution Single Look Complex SAR images; for the second approach the analysis is performed over detected SAR images over the same geographical area; after the formation of the patch database by applying a regular grid over the data, the Wigner-Ville spectrum is computed in a patch-wise approach and normalized to meet the requirements of a probability distribution;

next, the α-parameterized Rényi entropy is computed for each patch and normalized for clustering purposes;the scene is recomposed from the normalized coefficients and the classification map is generated.

5. On the applicability of the Rényi entropy to the TFR

The key step in the processing chain is the computation of the TF representation and the verification of constraints. In order for the Rényi entropy to be defined for the TF representation, as given in equation 3, the double integral has to be defined. Thus the condition that is imposed for the TFR is that

$$\iint C_s^{\alpha}(t,f)dtdf > 0 \tag{8}$$

For some classes of signals the above condition is not met and the Rényi entropy is not applicable. However, as shown in [13], the Rényi entropy of order 3 is well defined for a large range of signals. Moreover, Gaussian smoothing of the TFR with small kernels can be employed to resolve these issues. To check for these consistency requirements, we performed a statistical analysis over the patch database to verify that the computed TFR meets the positivity constraint. Fig. 2 gives an example of the TFR over a patch, and it's smoothed version with a Gaussian filter of kernel size 5. The spectrum is depicted both as an image and as a 3-D surface. The results show that there are no dominant negative peaks, at least in the smoothed version, which allows for the applicability of the Rényi entropy.

6. Working with discrete signals

In the experiments we employed a pre-normalized version of the TFR, in other words, the expression under the double integral in equation 3 is divided by the integral over the time and frequency domains of the TFR. This is equivalent to normalizing the signal energy. The Renyi entropy of order α becomes:

$$H_{\alpha}(C_s) = \frac{1}{1-\alpha}\log_2 \iint \left(\frac{C_s(t,f)}{\iint C_s(u,v)dudv} \right)^{\alpha} dtdf \tag{9}$$

Since the signal under analysis is discrete, with a finite number of samples, with the signal sampling given by the pulse repetition frequency (PRF) the formula for the Rényi entropy in the discrete case can be written as:

$$H_{\alpha}(C_s[n,k]) = \frac{1}{1-\alpha}\log_2 \sum_n \sum_k \left(\frac{C_s[n,k]}{\sum_u \sum_v C_s[n,k]} \right)^{\alpha} \tag{10}$$

7. Computation of the Rényi Coefficients Maps. Classification results

The discrete Rényi entropy was computed over the previously obtained patch databases, formed of complex and detected patches. The varying parameter was α, which was set to the values 3, 5 and 7. These values were selected in order to test whether or not the value of the parameter should be limited to α=3, or if other values of α can provide good estimates of the information content of the patches and thus could be used as descriptors of the patch. After the computation of the values of the Rényi entropy for the TF representation of each patch, the original SAR scene could be reconstructed. Fig. 5 depicts the results obtained for the two databases. The images marked as (a) depict the normalized Rényi coefficient maps for different values of the parameter α. The ones marked as (b) depict the classification maps obtained after a K-means classification of the coefficients maps, with a number of clusters equal to 5. Fig. 3**Error! Reference source not found.** shows the statistics of the values of the Rényi coefficients corresponding to the classes obtained by a binary classification: "Urban Area" and "Green Area". Three values of the α parameter were considered: 3, 5, and 7. The numbers in table 1 confirm the expected values of the Rényi entropy.

Table 1

Statistics of the Rényi coefficients for binary classification

α value/ database	Urban		Vegetation	
	Mean	Variance ($\cdot 10^{-3}$)	Mean	Variance ($\cdot 10^{-3}$)
α=3 , complex	4.56	1.8	4.69	3.1
α=3 , detected	4.26	0.72	4.33	0.93
α=5 , complex	2.30	0.58	2.37	0.94
α=5 , detected	2.13	0.18	2.16	0.23
α=7 , complex	1.53	0.26	1.58	0.42
α=7 , detected	1.42	0.08	1.44	0.10

We mentioned previously that the areas with increased heterogeneity should exhibit larger values of the entropy. This is true in the case where the entropy is computed directly on the image's pixels values, in other words directly on the image histogram.

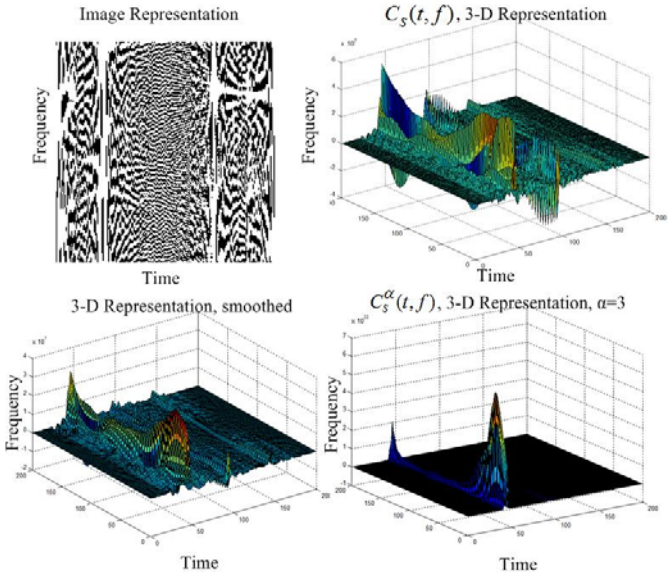

Fig. 2. Example of TF representation of a complex patch

Fig. 2 shows: (left to right) the representation of the Wigner-Ville spectrum as an image, as a 3-D surface, the smoothed version with a Gaussian filter and the 3-D representation of the TF representation, $C^{\alpha}{}_{S}(t,f)$ required for the double integral condition; no dominant negative peak is noticeable.

In our analysis, due to the fact that the entropy is computed on the image spectrum rather than on the image histogram, the entropy is an indicator or the spectrum homogeneity. It is expected that the areas covered with vegetation should have more uniform spectra, which in information theory terms translates into less information. Consequently, the entropy will be higher. In opposition to this, the urban areas will have more pronounced spectra, which will lead to a decrease of the values of the entropy. This fact is shown in table 1 where it can be seen that the entropy of the urban areas is lower than the entropy of the green areas in all the six considered cases (for both databases and for the three values of the alpha parameter).

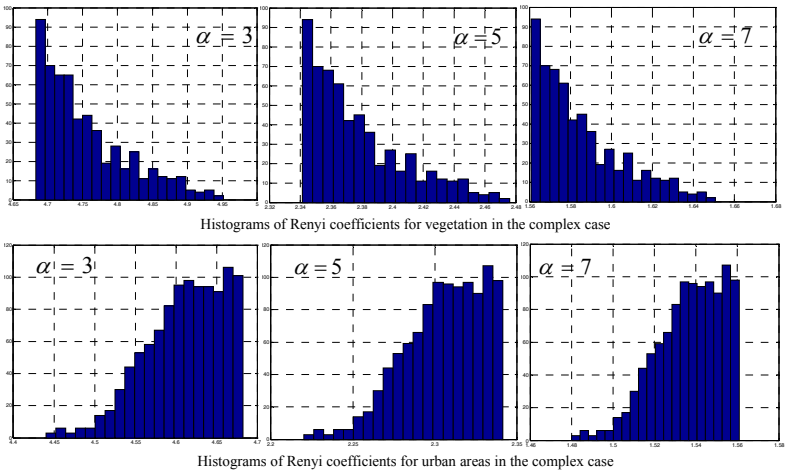

Fig. 3. Histograms of Rényi coefficients computed for the complex database, for binary classification: urban areas and vegetated areas

Fig. 3 depicts the distributions of the values of the Rényi entropies as functions of the alpha parameter and the considered classes. By analyzing the numbers in table 1 we can see that both the mean value and the variance of the entropy decrease with α. Although in all of the six considered cases all coefficient maps seem to discriminate between the vegetated and urban areas, the classification results (Fig. 5b) prove that not all coefficient maps have the same discriminative properties. Lower values of α (3 and 5) seem to give better classification results. Comparing the results obtained between the single look complex and detected databases, it appears that the complex signal contains more information than the amplitude signal, and this increased information is useful for scene classification. The most visible result is the case of α=7, where for the detected database the most distinctive class is formed of areas covered by vegetation, although the precision is visibly lower than for smaller values of α.

A first assessment was performed through visual inspection of the results. An example is given in Fig. 4, which shows the optical projection of the analyzed area, and the overlays of the vegetation masks obtained from the complex and detected databases over the optical image. The results show the precision is increased when the complex signal is employed. The false alarm rate is much higher in the detected case. Although in all of the six considered cases all coefficient maps seem to discriminate between the vegetated and urban areas, the classification results (Fig 5b) prove that not all coefficient maps have the same discriminative properties. Lower values of α (3 and 5) seem to give better classification results. Comparing the results obtained between the two databases, it appears that the complex signal contains more information than the amplitude signal, and this increased information is useful for scene classification. The most

visible result is the case of α=7, where for the detected database the most distinctive class is formed of areas covered by vegetation, although the precision is visibly lower than for smaller values of α.

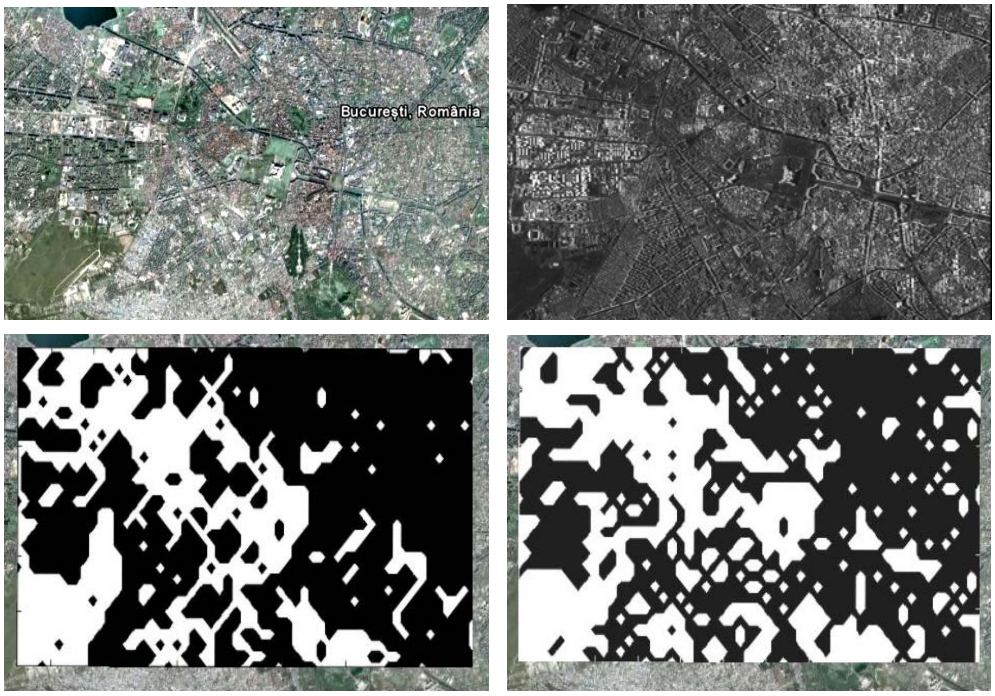

Fig. 4. (upper): optical Google Earth projection of the analyzed area, original SAR image, and (lower): the overlays of the vegetation masks obtained from the complex and detected databases over the optical image, for alpha = 3

8. Validation of Method

Table 2 shows a comparative result of the Single Look Complex and Detected databases and complements the results presented in Fig. 4.

By analyzing the precision, recall and accuracy values, one can state that for the detected database the best results are obtained by using the Rényi entropies parameterized by α=3. The table shows mean values of precision, recall and accuracy. The quality of the classification improves if the SLC database is employed. The maximum precision however is obtained for the Rényi entropy parameterized by α=5 for the class “Continuous Urban Fabric”.

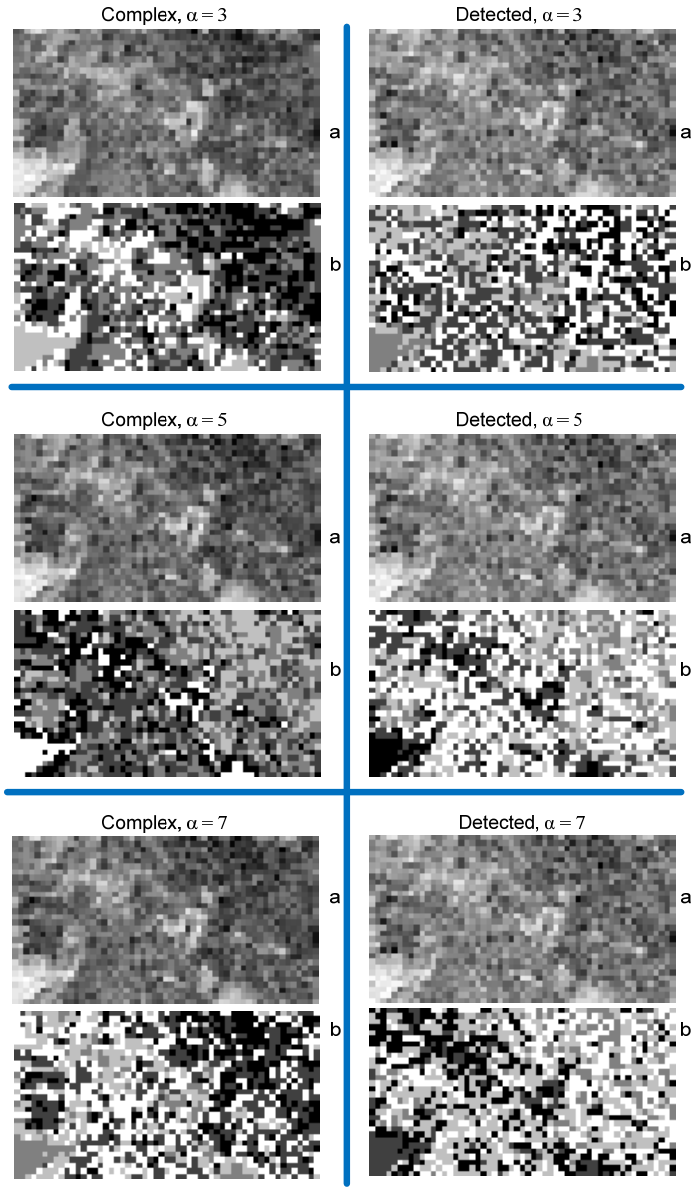

Fig. 5. (a) depicts the normalized Rényi coefficient maps for different values of the parameter α. The ones marked as (b) depict the classification maps obtained after a K-means classification of the coefficients maps, with a number of clusters equal to 5

Given the fact that the analyzed area comprises mostly densely populated areas in which the living facilities are mostly apartment blocks with very similar architecture, the number of patches in the database was very large. Thus, there is

little variability in the class which makes it easier to retrieve compared to other more heterogeneous classes. Hence, we can state that with the increased resolution, the phase information becomes important even with single band data.

Table 2

Mean Precision and Recall for classification on 16 annotated classes using Renyi coefficients

Alpha	Complex			Detected		
	Precision (mean) %	Recall (mean) %	Accuracy (mean) %	Precision (mean) %	Recall (mean) %	Accuracy (mean) %
3	44.80	41.68	94.50	43.20	40.71	94.18
5	46.81	41.53	94.47	40.18	39.70	94.06
7	43.92	40.91	94.22	45.51	39.02	94.22

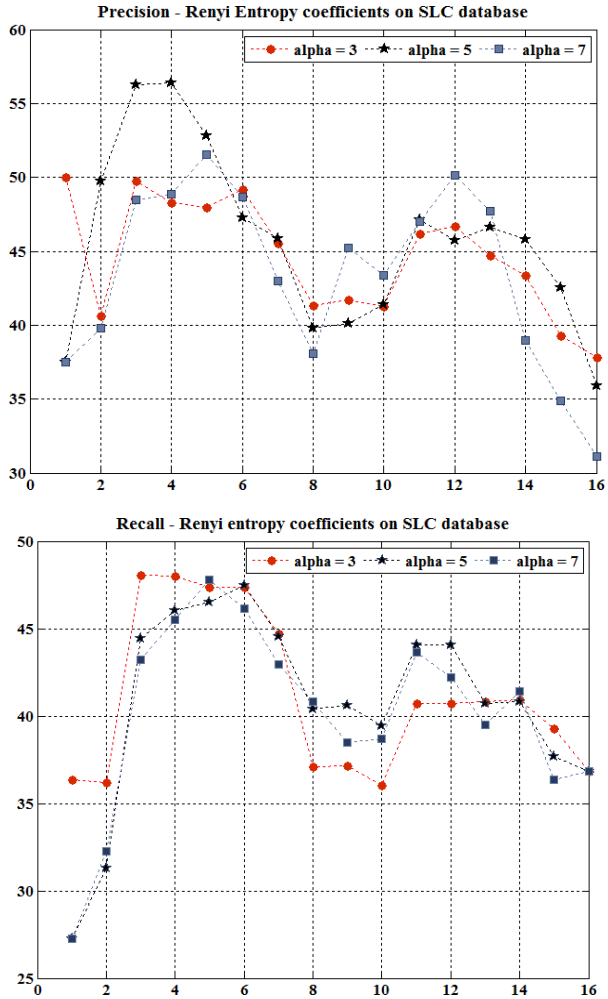

Fig. 6 Precision (left) and Recall (right) of classification using the Renyi Entropy parameterized by α= 3, 5 and 7 on complex database;

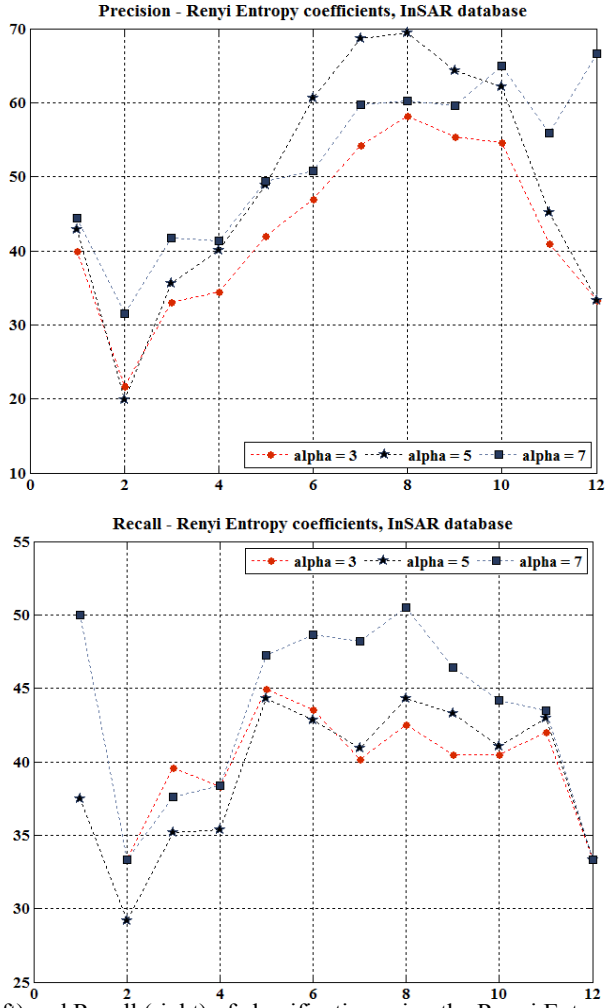

Fig. 7 Precision (left) and Recall (right) of classification using the Renyi Entropy parameterized by α= 3, 5 and 7on interferometric database;

Figs. 6, 7 and 8 present the Precision and Recall graphs for the Single Look Complex and Interferometric databases. The graphs depict the results obtained for the selected values of alpha. The Rényi entropy is parameterized by α=3, 5, 7. By analyzing the graphs, one can conclude that a value of α=5 would be preferred in the case of SLC data, while for interferometric data α=7 would yield better results. Overall, a number of 8 classes can be discriminated based on the Rényi Entropy of the patches spectra using the SLC database, with precision higher than 45%. On the other hand, by using the interferometric database, the number of identifiable classes increases to 11 (with precision higher than 45%).

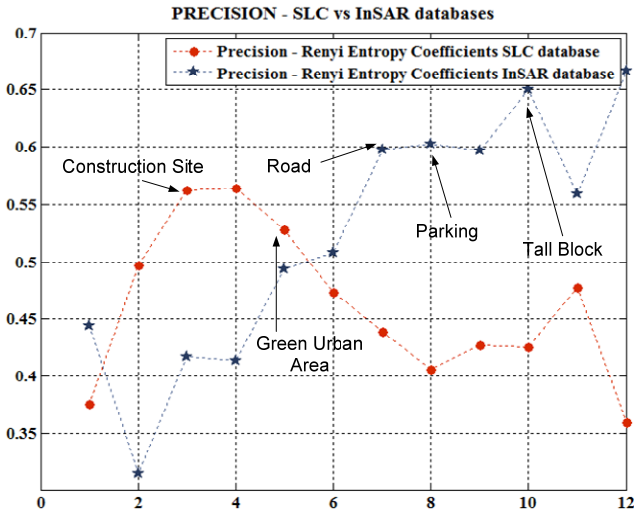

Fig. 8 Comparison of precision of classification obtained on Single Look Complex patches and Interferometric patches

The usage of interferometric information increases the precision in the case of coherent targets, such as buildings or roads. Areas with high dynamics and low coherence between acquisitions are better discriminated by SLC data.

9. Conclusions

In this paper we introduced the Rényi entropies of the TF representations as a descriptor for scene classification in a patch-wise approach. The most important properties of the Rényi entropies were presented and the applicability of the entropies on the Wigner-Ville representations of SAR signals was discussed. The tests were performed on three annotated databases, consisting of detected, single look complex and interferometric SAR data. The results show that the complex data adds value to the classification in the case of increased resolution. Moreover, interferometric data was proven to be better suited for urban classes' identification. The Rényi entropies were parameterized with α=3, 5, and 7. A lower value of α is required for good classification of detected SAR data, while larger values are required when the phase information is taken into account. A number of 8 classes were identified with precision higher than 45% using SLC data with Rényi entropies of order α=5. Adding the interferometric information allowed to increase the number of classes to 11.

R E F E R E N C E S

1] *V.S. Frost, K. S. Shanmugan* „The Information Content of Synthetic Aperture Radar Images of Terrain", IEEE Transactions on Aerospace and Electronic Systems, vol AES-19, no 5, Sept 1983

[2] *L. Alparone, B. Aiazzi, S. Baronti, A. Garzelli* „An Information-Theoretic Feature for Multi-temporal Analysis of SAR Images", Proceedings of ESA-EUSC 2006

[3*] M. Aragone, A. Caridi, S. B. Serpico, G. Moser, D. Cerra, M. Datcu* „Study of Information Content of SAR Imges", Proceedings of 2008 IEEE Radar Conference, pp 1-6, ISBN: 978-1-4244-1538-0, Rome, Italy, May 2008

[4] *B. Aiazzi, L. Alparone, S. Baronti, M. Bianchini, A. Garzelli, M. Selva* „Information Mining via Coherence Estimation from Multi-look Incoherent SAR Imagery", Proceedings of ESA-EUSC 2005

[5] *L. Bruzzone, D. Fernandez Prieto, S. B. Serpico* „A Neural-Statistical Approach to Multitemporal and Multisource Remote-Sensing Image Classification", IEEE Transactions on Geoscience and Remote Sensing, vol 37, no 3, May 1999, pp 1350-1359

[6] *R. J. Dekker* „Texture Analysis and Classification of ERS SAR Images for Map Updating of Urban Areas in The Netherlands", IEEE Transactions on Geoscience and Remote Sensing, vol 41, no 9, Sept 2003, pp 1950 – 1958

[7] *S. R. Cloude, E. Pottier* "An Entropy Based Classification Scheme for Land Applications pf Polarimetric SAR", IEEE Transactions on Geoscience and Remote Sensing, vol 35, no 1, Jan 1997, pp 68-78

[8] *Jong-Sen Lee, M. R. Grunes, T. L. Ainsworth, Li-Jen Du, D. L. Schuler, S. R. Cloude* "Unsupervised Classification using Polarimetric Decomposition and the Complex Wishart Classifier", IEEE Transactions on Geoscience and Remote Sensing, vol 37, no 5, Sept 1999, pp 2249-2258

[9] *S. Gabarda, G. Cristobal, P. Rodriguez, C. Miravet, J. M. del Cura* "A new Rényi Entropy-based Local Image Descriptor for Object Recognition", Proceedings of SPIE, vol 7723, DOI: 10.1117/12.854901, pp 772312-772312-13 (2010)

[10] *R. Jenssen, K. E. Hild II, D. Erdogmus, J. C. Principe, T. Eltoft* "Clustering using Rényi's Entropy ", Proceedings of the International Joint Conference on Neural Networks, vol 1, July 2003, ISSN; 1098-7576, pp 523-528

[11] *Yun He, A. B. Hamza, H. Krim* "A Generalized Divergence Measure for Robust Image Registration", IEEE Transactions on Signal Processing, vol 51, no 5, May 2003, pp 1211 – 1220

[12] *A. Popescu, I. Gavat, M. Datcu* "SAR Time-frequency Information Extraction based on Rényi Entropy", Proceedings of IWCIT 2008, Gliwice, Poland, Sept 2008, pp 201-206

[13] *R. G. Baraniuk, P. Flandrin, A. J.E.M. Janssen, O. J.J. Michel* "Measuring Time-Frequency Information Content using the Rényi Entropies", IEEE Transactions on Information Theory, vol 47, no 4, May 2001, pp 1391-1409

[14] *P. Flandrin, "Temps-Fréquence*", Traité des Nouvelles Technologies, série Traitement du Signal, Hermès, Paris, 1993, ISBN 2-86601-387-5, pp 224-290